

Crystalline Hybrid Solid Materials of Palladium and Decamethylcucurbit[5]uril as Recoverable Precatalysts for Heck Cross-Coupling Reactions

Hongfang Li,^[a] Jian Lü,^[a, b] Jingxiang Lin,^[a] Yuanbiao Huang,^[a] Minna Cao,^[a] and Rong Cao*^[a]

Abstract: A series of M–Pd–Me₁₀CB[5] (M=Li, Na, K, Rb, and Cs; Me₁₀CB[5]=decamethylcucurbit[5]uril) hybrid solid materials have been successfully synthesized for the first time through a simple diffusion method. These as-prepared hybrid solids have been applied as phosphine-free precatalysts for Heck cross-coupling reactions with excellent catalytic performance and good recyclability. In the

processes of the catalytic reactions, the activated Pd^{II} species were released from the crystalline hybrid precatalysts and transformed into catalytically active Pd nanoparticles, which have been demonstrated as key to carry on

the catalytic reactions for the recoverable precatalysts M–Pd–Me₁₀CB[5] (M=K, Rb, and Cs). It has also been rationalized that the introduction of different alkali metals afforded crystalline hybrid precatalysts with different crystal structures, which are responsible for their diversified stability and reusability presented in Heck reactions.

Keywords: cross-coupling · cucurbiturils · Heck reaction · nanoparticles · palladium

Introduction

The palladium-catalyzed Heck reaction that is, the arylation or vinylation of olefins, is one of the most important C–C coupling reactions in the pharmaceutical, agrochemical, and fine-chemical industries.^[1] Typically, ligand-free palladium salts or organometallic complexes with special ligands, for example phosphine, were generally used as palladium catalyst precursors in traditional Heck reactions.^[1–3] It has been observed that the palladium salts being used as homogenous catalysts generally suffer difficulties in separation, recycling, and deactivation caused by the aggregation of Pd species formed in situ during the Heck reaction;^[2,3] whereas most of the ligands of palladium organometallic complex catalysts are sensitive to air and moisture and are not stable enough in practical operation for industrial application.^[1] It is therefore desirable to develop a new catalytic system for Heck reactions that exhibits the dual advantages of high catalytic efficiency and good recyclability.

It has long been known that the judicious selection of organic ligands in palladium complexes is crucial for C–C coupling reactions because the catalytic activities, selectivity, and stability of metal complex catalysts are dictated by the steric and electronic characters of ligands as well as the properties of the metal–ligand coordination.^[4–7] Recently, N-heterocyclic carbenes (NHCs) have been used as alternative substitution of phosphine ligands to construct palladium complexes that exhibit high catalytic activities and chemical selectivity in the C–C coupling reaction. Such palladium complexes were air and moisture stable and could be recycled a reasonable number of times.^[8] However, the synthetic procedure for the ligands of NHCs is long and laborious. In this context, the development of suitable and facile non-phosphine ligands to construct palladium complexes as recoverable catalysts is one of the contemporary themes in C–C coupling reactions.

Cucurbit[*n*]urils (CB[*n*]) represent a family of homologues of organic macrocycles composed of *n* glycoluril monomers linked by 2*n* methylene bridges.^[9] CB[*n*] bears a pumpkin-shaped, rather rigid, and high symmetry structure featuring an open hydrophobic cavity fringed with two identical hydrophilic carbonylated portals.^[10] The structural rigidity along with the capability of forming stable complexes with organic molecules and metal ions make CB[*n*]s attractive as building blocks for the construction of hybrid metal–organic complexes.^[11] Over the past decade, a wide range of metal ions, including alkali, alkaline earth metals, first row transition metals, and some lanthanides, has been found to be successful in the preparation of solid-state materials with CB[*n*].^[12,13] The outstanding recognition properties

[a] Dr. H. Li, Dr. J. Lü, Dr. J. Lin, Dr. Y. Huang, Dr. M. Cao, Prof. R. Cao
State Key Laboratory of Structural Chemistry
Institution Fujian Institute of Research on the Structure of Matter
Chinese Academy of Sciences, Fujian, Fuzhou 350002 (P.R. China)
Fax: (+86) 591-8379-6710
E-mail: rcao@fjirsm.ac.cn

[b] Dr. J. Lü
School of Chemistry, University of Nottingham
University Park, Nottingham NG7 2RD (UK)

Supporting information for this article is available on the WWW under <http://dx.doi.org/10.1002/chem.201301703>.

of CB[n]s have prompted the rapid development of exciting applications in the supramolecular synthetic, host–guest chemistry, medicinal and material science fields.^[14] However, the design of the catalysts is still a long-standing challenge in the supramolecular chemistry of CB[n]s.^[15] Recently, a few organometallic reactions promoted or catalyzed by CB[n]s have been published.^[16] But there is rare report on the synthesis and application of noble metal–CB[n]s crystalline hybrid catalysts to the best of our knowledge. Thus, the design and synthesis of noble metal–CB[n]s crystalline hybrid materials has practical and academic significance in view of both scientific exploration and finding functional materials with practical use in catalytic C–C coupling reactions.

The decamethyl derivative Me₁₀CB[5], first reported by the group of Stoddart,^[17] has a core structure similar to that of CB[5] with the outer surface of the barrel equator decorated with methyl groups. Moreover, Me₁₀CB[5] can be considered as one of the smallest members of the CB[n]s family and processes narrow portals and a low cavity volume. Due to the low cavity volume, the supramolecular/coordination chemistry of Me₁₀CB[5] is mainly targeted on its portals. On the other hand, Me₁₀CB[5] shows good solubility compared with other members of CB[n]s, and captured our attention because it is extremely promising for the preparation of hybrid complexes with noble metals in aqueous solutions. Herein, a series of Pd^{II}-containing hybrid solids, [Li₂(H₂O)₄(H₂O@Me₁₀CB[5])][PdCl₄]·4H₂O (**1**, Li–Pd–Me₁₀CB[5]), [Na₂(H₂O)₅(H₂O@Me₁₀CB[5])][PdCl₄]·5H₂O (**2**, Na–Pd–Me₁₀CB[5]), [K₂(H₂O)₃(H₂O)_{0.5}@Me₁₀CB[5]][PdCl₄] (**3**, K–Pd–Me₁₀CB[5]), [Rb₂(H₂O)₃·(H₂O)_{0.5}@Me₁₀CB[5]][PdCl₄] (**4**, Rb–Pd–Me₁₀CB[5]), [Cs₂(H₂O)₂(H₂O@Me₁₀CB[5])][PdCl₄] (**5**, Cs–Pd–Me₁₀CB[5]) have been successfully self-assembled from Me₁₀CB[5] and the palladium complex in the presence of the corresponding alkali metal ions. X-ray structural analyses show that the alkali metal cations coordinate to the carbonyl oxygen atoms at the Me₁₀CB[5] portals into various molecular capsules, which further interact with [PdCl₄]²⁻ anions through either coordinative bonds or supramolecular interactions. To the best of our knowledge, compounds **1–5** represent the first examples of crystalline hybrid materials of noble metals and CB[n]s. Consequently, the as-synthesized Pd–Me₁₀CB[5] hybrid materials were tentatively used as effective catalysts in Heck cross-coupling reactions. It has been found that the catalytic activities and the reusability of the solid-state materials are closely related with their crystal structures.

Results and Discussion

Single-crystal X-ray diffraction studies unambiguously confirmed the framework structures of the five compounds and a combination of elemental analyses and TGA measurements gave the formulae. Compounds **1–5** are built by alkali metal cations (Li⁺, **1**; Na⁺, **2**; K⁺, **3**; Rb⁺, **4**; and Cs⁺, **5**) and Me₁₀CB[5] moieties into various molecular capsules

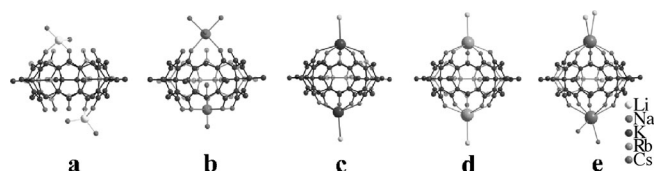


Figure 1. Coordination patterns of Me₁₀CB[5] with various alkali metal cations into molecular capsules.

(Figure 1); [PdCl₄]²⁻ anions appear as counteranions and interact by means of either supramolecular interactions or coordinative bonds.

Crystal structures of compounds 1–5: In the structure of compound **1**, [Li₂(H₂O)₄(H₂O@Me₁₀CB[5])][PdCl₄]·4H₂O, two lithium cations bind to a Me₁₀CB[5] molecule into a "half-open" molecular capsule due to the small atomic radii of Li⁺ (Figure 1 a) with one uncoordinated water molecule being encapsulated inside the molecular capsule. The tetrahedral coordination sphere of Li⁺ is defined by two aqua ligands and two carbonyl oxygen atoms from a Me₁₀CB[5] unit. One aqua ligand on a lithium cation interacts with an adjacent (Li₂Me₁₀CB[5]) molecular capsule in a mutual fashion, resulting in a one-dimensional (1D) supramolecular chain structure (Figure 2). The [PdCl₄]²⁻ anions in compound **1** are located on one side of the 1D supramolecular chain through the weak coordination of palladium centers to the aqua ligands (Pd–O, 3.347(2) Å) that are involved in intra-chain H-bond interactions (Figure 2).

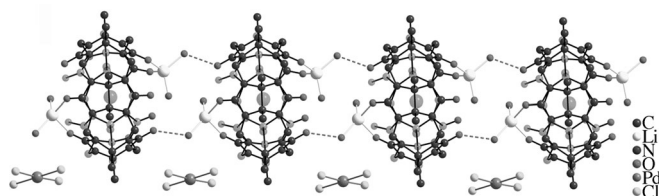


Figure 2. A view of the 1D supramolecular chain structure in compound **1**.

Two crystallographically independent sodium cations in the compound [Na₂(H₂O)₅(H₂O@Me₁₀CB[5])][PdCl₄]·5H₂O (**2**) bond unevenly to each portal of a Me₁₀CB[5] unit to form a "half-closed" molecular capsule (Figure 1 b). The octahedral Na(1) center is coordinated by two carbonyl oxygen atoms and four aqua ligands at one portal, whereas Na(2) is surrounded by all five carbonyl atoms of the other portal and two apical aqua ligands into a pentagon bi-pyramid coordination geometry. Adjacent (Na₂Me₁₀CB[5]) molecular capsules are connected through the H-bonds formed between the aqua ligands on the octahedral sodium centers and the carbonyl oxygen atoms at the equatorial positions of pentagon bi-pyramidal sodium centers, giving rise to 1D supramolecular bi-chains (Figure 3). The [PdCl₄]²⁻ anions and uncoordinated water molecules appear in the crystal lattice involving in complicated H-bond interactions and form the

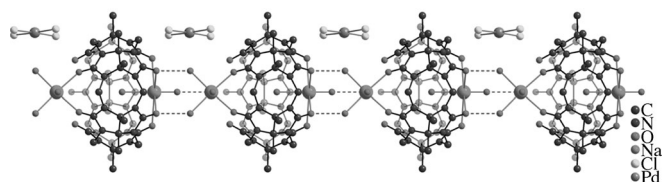


Figure 3. A view of the 1D supramolecular chain structure in compound **2**.

overall three-dimensional (3D) supramolecular structure of compound **2**.

The potassium and rubidium cations form isostructural compounds with $\text{Me}_{10}\text{CB}[5]$ and $[\text{PdCl}_4]^{2-}$ anions with a general formula of $[\text{M}_2(\text{H}_2\text{O})_3\{(\text{H}_2\text{O})_{0.5}\text{@Me}_{10}\text{CB}[5]\}][\text{PdCl}_4]$ ($\text{M}=\text{K}$, **3**; Rb , **4**), and thus only the structure of potassium-containing compound **3** is discussed in detail. Two K^+ cations are capped at each portal of a $\text{Me}_{10}\text{CB}[5]$ to form the closed molecular capsule (Figure 1c), which is one of the most common features observed for potassium-cucurbit[n]uril ($n=5$ or 6) coordination compounds.^[18] A half-uncoordinated water molecule appears in each $(\text{K}_2\text{Me}_{10}\text{CB}[5])$ molecular capsule and the neighboring capsules are joined together by the $[\text{PdCl}_4]^{2-}$ anions by means of the coordination of K^+ centers to the chlorine atoms of the $[\text{PdCl}_4]^{2-}$ anions. In such a way, a 1D coordination chain subunit is formed (Figure 4). The 1D chain subunits are further ex-

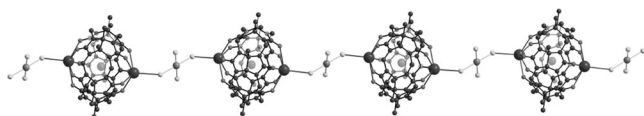


Figure 4. A view of the 1D coordination chain subunit in compound **3**.

tended into two-dimensional (2D) grid layer through the connection of two potassium centers at different molecular capsules by sharing the aqua ligands, as shown in Figure 5. Uncoordinated water molecules exist in the crystal lattice and interact with the coordination network through extensive H-bond interactions.

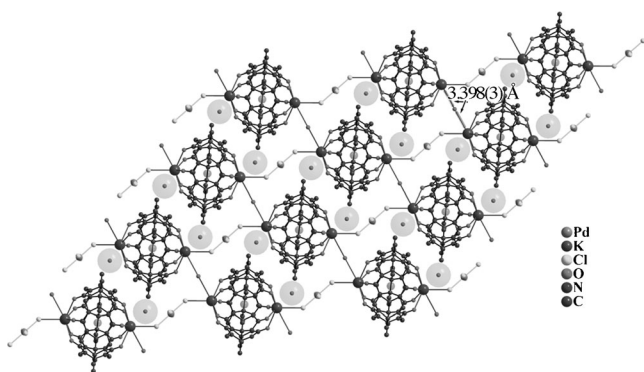


Figure 5. A view of the 2D supramolecular layer structure in compound **4**.

The closed molecular capsule ($\text{Cs}_2\text{Me}_{10}\text{CB}[5]$) is also found in cesium-containing compound **5**, $[\text{Cs}_2(\text{H}_2\text{O})_2\{\text{H}_2\text{O}@Me_{10}\text{CB}[5]\}][\text{PdCl}_4]$, by means of capping two Cs^+ cations to both portals of a $\text{Me}_{10}\text{CB}[5]$ (Figure 1e). The anionic species $[\text{PdCl}_4]^{2-}$ coordinates to the *exo* position of a Cs^+ on one side to form a decorated molecular capsule $[\text{Pd}\{\text{Cs}_2\text{Me}_{10}\text{CB}[5]\}]$, which interacts by means of hydrogen-bonding interactions to give a supramolecular chain subunit (Figure 6). A 3D supramolecular net is comprised through complicated H-bonds present ($\text{O}_{\text{carbonyl}}\cdots\text{O}_{\text{w}}$, 2.900(1) Å, 2.917 Å; $\text{O}_{\text{w}}\cdots\text{O}_{\text{w}}$, 2.581(3) Å).

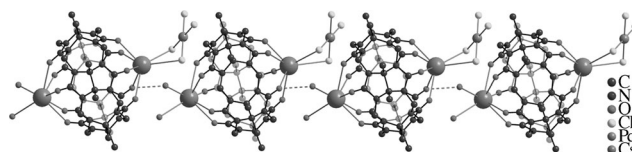


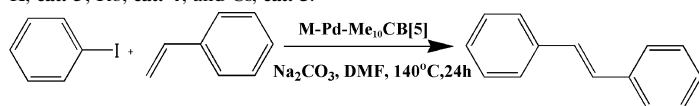
Figure 6. A view of the 2D supramolecular chain structure in compound **5**.

Powder X-ray diffractions (PXRD) and thermogravimetric analyses (TGA): The phase purity and homogeneity of the as-synthesized bulk products of compounds **1–5** were identified by using PXRD at room temperature. The experimental PXRD patterns of samples **1–5** are in good agreement with the ones simulated from single crystal X-ray diffraction data (Figures S1–S4, the Supporting Information), which clearly indicates the purity and homogeneity of the five compounds.

TGA were recorded in the temperature range of 20–900 °C to investigate the thermal stability of compounds **1–5** as well as the determination of water molecules present in each compound. The TGA curves of compounds **1** and **2** (Figure S5, the Supporting Information) showed similar continuous weight losses between 30 and 250 °C, corresponding to the release of uncoordinated and coordinated water molecules (9 water molecules for **1**, calcd: 11.2; found: 11.6%; 11 water molecules for **2**, calcd: 13.5; found: 13.9%). Compounds **1** and **2** underwent further weight losses from 250 (for **1**) and 300 °C (for **2**), respectively, which was assigned to the decomposition of the organic components. Compounds **3–5** displayed first step of weight losses before 200 °C, which corresponded to the loss of water molecules (3.5 water molecules for **3**, calcd: 4.6; found: 4.5%; 3.5 water molecules for **4**, calcd: 4.3; found: 3.6%; 3 water molecules for **5**, calcd: 3.5; found: 3.35%). Further weight losses of compounds **3–5** appeared at higher temperatures, compared with compounds **1** and **2**, around 400 °C due to the release of organic $\text{Me}_{10}\text{CB}[5]$.

Catalytic performance in Heck coupling reactions: The Pd-containing hybrid solid materials **1–5** were tentatively exploited as catalysts (denoted as $\text{M-Pd-Me}_{10}\text{CB}[5]$; $\text{M}=\text{Li}$, **cat.-1**; Na , **cat.-2**; K , **cat.-3**; Rb , **cat.-4**; and Cs , **cat.-5**) for Heck reactions. In this current system, Heck reaction of iodobenzene with styrene was chosen as a model reaction. Reaction conditions, including base species, solvents, and tem-

Table 1. The Heck reaction of iodobenzene and styrene catalyzed by M–Pd–Me₁₀CB[5] catalysts.^[a] M–Pd–Me₁₀CB[5]; M=Li, **cat.-1**; Na, **cat.-2**; K, **cat.-3**; Rb, **cat.-4**; and Cs, **cat.-5**.



Entry	Catalysts	Amount [mol %]	Yield [%]
1	K–Pd–Me ₁₀ CB[5] (cat.-3)	0.5	86 ^[b]
2	cat.-3	1.0	90 ^[b]
3	cat.-3	2.0	85 ^[b]
4	cat.-3	3.0	73 ^[b]
5	Li–Pd–Me ₁₀ CB[5] (cat.-1)	1.0	81 ^[c]
6	Na–Pd–Me ₁₀ CB[5] (cat.-2)	1.0	83 ^[c]
7	cat.-3	1.0	82 ^[c]
8	Rb–Pd–Me ₁₀ CB[5] (cat.-4)	1.0	85 ^[c]
9	Cs–Pd–Me ₁₀ CB[5] (cat.-5)	1.0	86 ^[c]
10	[Li ₂ PdCl ₄]	1.0	89 ^[b]
11	[Na ₂ PdCl ₄]	1.0	91 ^[b]
12	[K ₂ PdCl ₄]	1.0	89 ^[b]
13	[Li ₂ PdCl ₄]/Me ₁₀ CB[5] ^[d]	1.0	92 ^[b]
14	[Na ₂ PdCl ₄]/Me ₁₀ CB[5] ^[d]	1.0	93 ^[b]
15	[K ₂ PdCl ₄]/Me ₁₀ CB[5] ^[d]	1.0	92 ^[b]
16	[K ₂ PdCl ₄] ^[e]	1.0	31 ^[b]
17	[K ₂ PdCl ₄]/Me ₁₀ CB[5] ^[e]	1.0	42 ^[b]
18	[Na ₂ PdCl ₄] ^[e]	1.0	26 ^[b]
19	[Na ₂ PdCl ₄]/Me ₁₀ CB[5] ^[e]	1.0	38 ^[b]

[a] Reaction conditions: aryl halides (1 mmol), olefin (1.5 mmol), Na₂CO₃ (2 mmol), DMF (3 mL), M–Pd–Me₁₀CB[5] catalysts (0.5–1.0 mol %). [b] Yield determined by using GC (dodecane as internal standard); [c] Yield of the isolated product. [d] The mixture of [M₂PdCl₄]/Me₁₀CB[5]. [e] The reuse of catalysts for a second time.

perature, were monitored and determined (Table 1). A series of time-controlled experiments have been performed to determine the reaction time and the results are listed in Figure S6 (the Supporting Information). As can be seen, after reaction for 16 h, the product yields all have no dramatic change. However, considering some other substrates need higher energy to promote the Heck reaction, the heating period was fixed at 24 h in our work. Besides, the optimized catalyst loading was initially screened with the K–Pd–Me₁₀CB[5] catalyst in the range of 0.5 to 3.0 mol %, showing the best catalytic GC yield at 1.0 mol % (Table 1 entries 1–4). Therefore, 1.0 mol % of catalyst loading was applied for all the M–Pd–Me₁₀CB[5] catalysts. Despite of the different alkali metals in the crystalline hybrid solids, the M–Pd–Me₁₀CB[5] catalysts exhibit similar catalytic activity in the coupling reactions of iodobenzene and styrene with good yields (80–85 %, Table 1, entries 5–9).^[19] For comparison, [M₂PdCl₄] (M=Li, Na, and K) and the mixture of [M₂PdCl₄]/Me₁₀CB[5] have also been used as catalysts in the model Heck reaction (Table 1, entries 10–15). It is clear to see that the obtained yields with the crystalline catalysts are comparative with the corresponding homogeneous [M₂PdCl₄] and [M₂PdCl₄]/Me₁₀CB[5] mixture catalysts.

Table 2. Heck coupling reactions catalyzed by K–Pd–Me₁₀CB[5].^[a]

Entry	Ar–X	R	Yield [%] ^[b]
1	C ₆ H ₅ I	C ₆ H ₅	82
2	C ₆ H ₅ Br	C ₆ H ₅	84
3	4-MeOC ₆ H ₄ I	C ₆ H ₅	84
4	4-MeOC ₆ H ₄ Br	C ₆ H ₅	82
5	4-NO ₂ C ₆ H ₄ Br	C ₆ H ₅	85
6	4-CNC ₆ H ₄ Br	C ₆ H ₅	88
7	4-MeCOC ₆ H ₄ Br	C ₆ H ₅	90
8	4-CF ₃ C ₆ H ₄ Br	C ₆ H ₅	84
9	C ₆ H ₅ I	CO ₂ <i>n</i> Bu	99
10	C ₆ H ₅ I	CO ₂ <i>t</i> Bu	75
11	C ₆ H ₅ I	CO ₂ Me	80
12	C ₆ H ₅ Br	CO ₂ <i>n</i> Bu	95
13	C ₆ H ₅ Br	CO ₂ <i>t</i> Bu	70
14	C ₆ H ₅ Br	CO ₂ Me	85
15	4-MeOC ₆ H ₄ I	CO ₂ <i>n</i> Bu	99
16	4-MeOC ₆ H ₄ I	CO ₂ <i>t</i> Bu	88
17	4-MeOC ₆ H ₄ I	CO ₂ Me	82
18	4-MeOC ₆ H ₄ Br	CO ₂ <i>n</i> Bu	96
19	4-MeOC ₆ H ₄ Br	CO ₂ <i>t</i> Bu	85
20	4-MeOC ₆ H ₄ Br	CO ₂ Me	87

[a] Reaction conditions: aryl halides (1 mmol), olefin (1.5 mmol), Na₂CO₃ (2 mmol), DMF (3 mL), and K–Pd–Me₁₀CB[5] catalyst (1.0 mol %). [b] Yield of the isolated product.

To explore the scope of the catalytic reactions, a series of aryl iodides/bromides with different olefins were examined by using 1.0 mol % K–Pd–Me₁₀CB[5] as the catalyst and the results are listed in Table 2. Despite the bond energy of C–Br being higher than C–I, the Heck reaction between iodobenzene and bromobenzene with styrene were carried out effectively and gave comparable yields of *trans*-stilbene (82 vs. 84.0 %, Table 2, entries 1 and 2). Moreover, substitutions with either electron-donating groups (–OMe) or electron-withdrawing groups (–NO₂, –CN, –CF₃, and –COCH₃) on the *para* position of iodobenzene (Table 2, entry 3) and bromobenzene (Table 2, entries 4–8) did not affect greatly the yield of the final products. The yields of the isolated products vary from 82 to 90 % with the best outcome for 4-MeCOC₆H₄Br with styrene coupling (90 %, Table 2, entry 7). In addition, various olefin derivatives with different ester substituents were applied to Heck reactions with iodobenzene/bromobenzene using K–Pd–Me₁₀CB[5] catalyst (Table 2, entries 9–14). It was found that the cross-coupling of aryl iodide/bromide with ester-substituted olefins successfully gave rise to the corresponding *trans*-configured products in excellent yields. The yields of aryl halides (95–99 %) with *n*-butyl acrylate were considerably higher than those with styrene, indicating that the electron-withdrawing groups on the substrates were favorable in the catalysis system (Table 2, entries 9 and 12). Notably, the yields decreased slightly when the *n*-butyl acetate group was replaced by methyl acetate (Table 2, entries 11 and 14), whereas the efficiency of the *tert*-butyl acetate-substituted olefin was obviously affected by its steric hindrance and gave lower yields (Table 2, entry 10 and 13). On the other hand, substitution of 4-me-

thoxyl groups on the halides generally increased the yields of coupling reactions with ester-substituted olefins (Table 2, entries 15–20).

Taking into consideration that the stability and reusability of catalysts are important for their practical applications, recycling Heck reactions of aryl iodides and styrene as coupling partners were carried out in the presence of M–Pd–Me₁₀CB[5] catalysts (**cat.-1–5**). After the first cycle, **cat.-1** and **cat.-2** catalysts lost crystallinity due to the structural decomposition (Figure S7 and S8, the Supporting Information) and were deactivated. However, **cat.-3–5** remained their crystallinity, intact structures (Figure 7, and S9 and

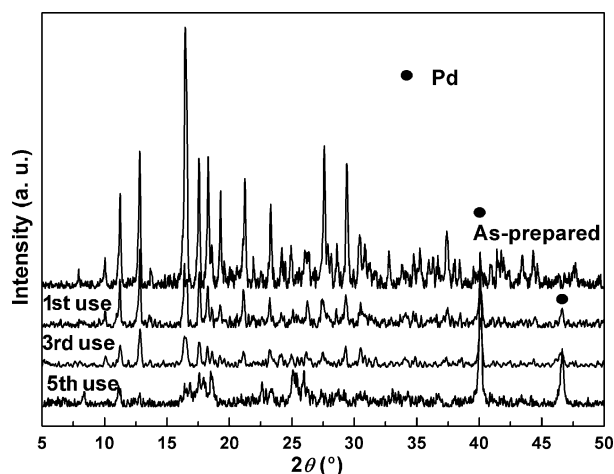


Figure 7. PXRD patterns of K–Pd–Me₁₀CB[5] during cycling reactions.

S10, the Supporting Information), as well as their catalytic effectiveness. Catalysts **cat.-3–5** could be easily recovered through centrifugation and reused in the coupling reactions under the same conditions for several consecutive runs. The yields of the isolated products of cyclic reactions using **cat.-3–5** only decreased slightly after five cycles (Table 3). For comparison, [M₂PdCl₄] and [M₂PdCl₄]/Me₁₀CB[5] mixed catalysts have also been reused. However, the yields decreased dramatically (Table 1, entries 16–19) in the second cycle and the catalysts deactivated gradually due to the aggregation of

Table 3. Cyclic use of M–Pd–Me₁₀CB[5] (M=K, Rb, and Cs) catalysts in the Heck reaction of iodobenzene and styrene.^[a]

Entry	Cycles	<i>t</i> [h]	K–Pd– Me ₁₀ CB[5]		Rb–Pd– Me ₁₀ CB[5]		Cs–Pd– Me ₁₀ CB[5]	
			<i>c</i> _{Pd} [ppm] ^[b]	Yield ^[c] [%]	<i>c</i> _{Pd} [ppm] ^[b]	Yield ^[c] [%]	<i>c</i> _{Pd} [ppm] ^[b]	Yield ^[c] [%]
1	1 st	24	30.0	82	40.4	85	21.3	86
2	2 nd	24	20.5	83	19.9	83	19.0	82
3	3 rd	24	12.9	83	10.3	82	13.8	81
4	4 th	24	6.4	82	2.9	79	5.1	79
5	5 th	24	3.5	78	1.8	76	3.6	77

[a] Reaction conditions: iodobenzene (1 mmol), styrene (1.5 mmol), Na₂CO₃ (2 mmol), DMF (3 mL), compounds **3–5** (1 mol%). [b] Metal concentration in the filtrate detected by using ICP. [c] Yield of the isolated product.

big Pd particles after the reaction (Figure S11, the Supporting Information). These results showed that M–Pd–Me₁₀CB[5] (M=K, Rb, and Cs) exhibited much better reusability over [M₂PdCl₄] and [M₂PdCl₄]/Me₁₀CB[5], although the catalytic behavior of these catalysts in the first cycle reaction are similar (see above).

In the process of the cyclic reactions with **cat.-3–5**, the recovered catalysts were examined by PXRD measurements. It was noticed that the diffraction line (111) of Pd⁰ could be clearly observed in the PXRD patterns and the intensity increased with the runs (Figure 7, S9 and S10, the Supporting Information) due to the in situ-formation of the Pd⁰ species during the Heck reactions with **cat.-3–5**. TEM was used to confirm the formation of Pd nanoparticles (NPs) with size smaller than 5 nm in these systems (Figure 8a and 8b) and

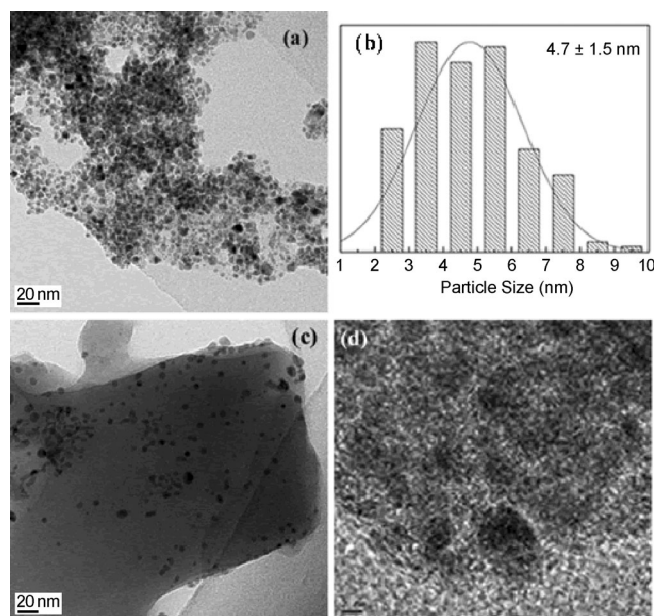


Figure 8. TEM images of palladium nanoparticles after (a) second and (c) fifth run of Heck reaction for K–Pd–Me₁₀CB[5]; (b) the corresponding size distribution and (d) HRTEM images of palladium nanoparticles in (a).

the high resolution TEM (HRTEM) images indicated that the Pd NPs possessed good crystallinity (Figure 8d). It is well-known that the Pd⁰ species formed in situ in the Heck reactions, especially in the homogeneous catalytic systems using ligand-free Pd precatalysts, which could be subject to two competing processes: one is to aggregate to form deactivated palladium black, which is the case of **cat.-1** and **cat.-2** (Figure S7 and S8, the Supporting Information), and the other process is to form catalytically active Pd NPs, as in the cases of **cat.-3–5**.^[20]

The alternative pathway is mainly determined by the local Pd^{II} concentration and its surroundings in the reaction system. As indicated in the previous work, the formation of palladium black could be effectively suppressed, whereas the palladium concentration was kept below 0.1 mol% (cor-

responding to ≈ 35.5 ppm).^[21] The inductively coupled plasma emission spectrometry (ICP) results of the filtrates with **cat.-1** and **cat.-2** showed Pd concentrations higher than 200 ppm after the first run, which were greatly higher than the threshold value (35.5 ppm), and thus the formation of palladium black was visible and the Heck reaction ceased in these two systems. However, the Pd concentrations slowly released from **cat.-3-5** were generally comparable or lower than 35.5 ppm (Table 3), and thus the formation of Pd-black could be dramatically suppressed. Moreover, the coordination effect of Me₁₀CB[5] to Pd species prevented the agglomeration for Pd⁰ species. Such synergistic effects actually lead to the formation of catalytically activated Pd NPs.

Although Pd NPs have been previously observed in Heck reactions catalyzed by Pd^{II} sources,^[22] it is not entirely clear as to whether the Pd NPs contribute in the catalytic activity. The concentrations of Pd species in filtrates were dramatically decreased following the third cycle (Table 3) and thus, if solely dependent on Pd species in reaction solution, one would expect the Heck reaction to proceed in very low yields. No dramatic decrease in yield is however observed at this point and it is thus proposed that the Pd NPs prolong the catalytic activity. The slight decrease in yield was observed following several successive cycles (Table 3) and it is postulated that this is due to an increase in Pd NP size (Figure 8c) and thus a decrease in surface area available for catalysis. Mechanistically, the hybrid catalysts **cat.-3-5** slowly release the Pd^{II} species (with detectable concentrations below 40 ppm) at the very initial period and catalyze the Heck reaction in a homogeneous fashion; the Pd^{II} species being released transform into Pd NPs and grow on the surface of solid catalysts **cat.-3-5**, which can be considered as a reservoir for the actual catalytically active Pd⁰ species at later stages in a heterogeneous fashion;^[23] the balancing between Pd^{II} being released and Pd⁰ attached to the surface of the solid catalysts plays a subtle role in the transfer from homogeneous to heterogeneous catalytic reactions. Thus the crystalline hybrid catalysts (**cat.-3-5**) function as precatalysts to launch the Heck cross-coupling reactions, at the same time, as supports for the actual catalytically active Pd NPs and carry on the reactions in a recyclable way. Different from the heterogeneous Pd nanoparticles immobilization on different supports,^[24] such Pd crystalline solids precatalysts possess high catalytic activity of homogeneous catalysts as well as good reusability of heterogeneous catalysts. Moreover, the in situ-generated Pd NPs can be stabilized by Me₁₀CB[5] ligand without addition of any surfactants or polymer to protect the Pd NPs from aggregations.

It is also reasonable that the M–Pd–Me₁₀CB[5] catalysts behave differently in the catalytic reactions from a structural point of view. In the structures of M–Pd–Me₁₀CB[5] (**cat.-1** and **cat.-2**) hybrid catalysts, the [PdCl₄]²⁻ anions interact with the (M₂Me₁₀CB[5]) molecular capsules through weak supramolecular H-bond interactions; whereas, in the structures of M–Pd–Me₁₀CB[5] (**cat.-3-5**) hybrid catalysts, the [PdCl₄]²⁻ anions covalently bound to the (M₂Me₁₀CB[5]) molecular capsules through stronger coordinative bonds.

Therefore, the release of the Pd^{II} species from **cat.-1** and **cat.-2** hybrid catalysts at the initial stage of the catalytic reactions was more easy than that from **cat.-3-5** and generated palladium black. Alternatively, the Pd releasing rates may also be responsible for the stability of the hybrid catalysts, that is, the slower the Pd releasing rate, the more stable the catalyst. Of note is that cucurbit[*n*]urils (CB[*n*], *n*=5–8) have been widely used in the fabrication of noble metal NPs in which the CB[*n*]s function as protecting agents.^[25] In this current catalytic systems, the Me₁₀CB[5] may play triple roles: 1) as a delivery vehicle to carry and release catalytically active Pd species to the Heck reaction systems; 2) as a regulator to control the releasing rate and concentration of Pd species from the crystalline hybrid precatalysts; 3) as a stabilizer to restrict the over-growth of the catalytically active Pd NPs.

Conclusion

A series of crystalline hybrid solid materials assembled from Me₁₀CB[5] and [PdCl₄]²⁻ anions in the presence of different alkali metal cations have been successfully synthesized for the first time by means of a simple diffusion method (M–Pd–Me₁₀CB[5]; M=Li, **cat.-1**; Na, **cat.-2**; K, **cat.-3**; Rb, **cat.-4**; and Cs, **cat.-5**). The as-synthesized hybrid solids have been examined as precatalysts for Heck cross-coupling reactions and indeed exhibited good catalytic activities of a wide range of reaction substrates. It has also been rationalized that the introduction of various alkali metals afforded diversified crystal structures of the hybrid precatalysts, which could be responsible for the different stability and reusability of the hybrid precatalysts in Heck reactions. In the process of the catalytic reactions, the catalytically active Pd species were released from the crystalline hybrid catalysts, delivered to the reaction systems, and then transformed into catalytic active Pd NPs. The hybrid precatalysts **cat.-3-5** could be easily recycled for several times through simple centrifugation, without dramatically losing their catalytic activities. In conclusion, the crystalline hybrid precatalysts **cat.-3-5** developed a new and unusual system for the C–C coupling reactions. Moreover, the synthesis of noble metal/Me₁₀CB[5] crystalline hybrid materials opened up a new direction for design of CB[*n*] catalysts in the supramolecular chemistry field.

Experimental Section

Materials and instrumentation: All chemicals were commercially purchased and used without purification. Me₁₀CB[5] was synthesized according to the process reported in the literature.^[26] Elemental analyses (C, H, and N) were carried on an Elementar Vario EL III analyzer. Metal analysis was determined by using an inductively coupled plasma emission spectrometer (ICP) Jobin Yvon Ultima 2. X-ray powder diffractions (XRPD) were performed with a Rigaku DMAX 2500 diffractometer. TGA was performed under a flow of nitrogen at a rate of 10 °C min⁻¹, by using a TA SDT-Q600 instrument. The TEM images were taken on

a FEI TECNAI G2 F20 microscope at an accelerating voltage of 200 kV. For TEM observations, the catalysts after catalytic reaction were ultrasonically dispersed in ethanol and deposited on the holey carbon film on a copper grid. The crude product yield of the catalytic reaction was determined by using Aligent 7890A gas chromatograph (GC) using dodecane as internal standard. The NMR spectra were measured on an Avance III Bruker Biospin spectrometer.

X-ray structure determinations: Single-crystal X-ray diffraction data of compounds **1** and **3** were collected on a Rigaku Saturn 70 (4×4 bin mode) diffractometer equipped with graphite monochromatized Mo_{Kα} radiation (λ=0.71073 Å) and a CCD area detector; the diffraction data of compounds **2** and **5** were collected on a Xcalibur, Eos diffractometer equipped with graphite monochromatized Mo_{Kα} radiation (λ=0.71073 Å); and the diffraction data of compound **4** was collected on a Mercury2 (1×1 bin mode) CCD diffractometer with graphite monochromatized Mo_{Kα} radiation (λ=0.71073 Å). Empirical absorption corrections were applied to the data using the Crystal Clear program.^[27] Structural solutions and full matrix least-squares refinements based on F² were performed with the SHELXS-97 and SHELXL-97 program packages, respectively.^[28] All of the non-hydrogen atoms were refined anisotropically. Crystal data and structure refinement parameters are given in Table S1 (the Supporting Information). CCDC-935991 (**1**), CCDC-935992 (**2**), CCDC-935993 (**3**), CCDC-935994 (**4**), and CCDC-935995 (**5**) contain the supplementary crystallographic data for this paper. These data can be obtained free of charge from The Cambridge Crystallographic Data Centre via www.ccdc.cam.ac.uk/data_request/cif.

General synthesis of compounds 1–5: Palladium chloride (30 mg, 0.17 mmol) was dissolved in concentrated HCl (0.5 mL), then distilled water (20 mL) was added to form a clear aqueous solution of [PdCl₄H₂] (solution I). Me₁₀CB[5] (100 mg, 0.1 mmol) and alkali metal chloride (0.2 mmol) were dissolved in distilled water (20 mL) under magnetic stirring (solution II). Solutions I and II were carefully transferred to each side of an H-tube, respectively. Orange crystals were obtained after several hours to up to three days in the H-tube by slow diffusion.

[Li₂(H₂O)₄(H₂O@Me₁₀CB[5])][PdCl₄·4H₂O (**1**): Yield: ≈75%, based on Me₁₀CB[5]; elemental analysis calcd (%) for C₄₀H₆₈N₂₀O₁₉Cl₄Li₂Pd: C: 34.4, H: 4.88, N: 20.1; found: C: 34.6, H: 4.80, N: 21.2.

[Na₂(H₂O)₃(H₂O@Me₁₀CB[5])][PdCl₄·5H₂O (**2**): Yield: ≈40%, based on Me₁₀CB[5]; elemental analysis calcd (%) for C₄₀H₇₂N₂₀O₂₁Cl₄Na₂Pd: C: 32.8, H: 4.9, N: 19.1; found: C: 32.1, H: 4.82, N: 19.0.

[K₂(H₂O)₃(H₂O)_{0.5}@Me₁₀CB[5]][PdCl₄] (**3**): Yield: ≈81%, based on Me₁₀CB[5]; elemental analysis calcd (%) for C₄₀H₅₇N₂₀O_{13.5}Cl₄K₂Pd: C: 35.3, H: 4.19, N: 20.6; found: C: 34.8, H: 4.21, N: 21.2.

[Rb₂(H₂O)₃(H₂O)_{0.5}@Me₁₀CB[5]][PdCl₄] (**4**): Yield: ≈51%, based on Me₁₀CB[5]; elemental analysis calcd (%) for C₄₀H₅₇N₂₀O_{13.5}Cl₄Rb₂Pd: C: 33.0, H: 3.92, N: 19.3; found: C: 33.0, H: 3.94, N: 20.2.

[Cs₂(H₂O)₂(H₂O@Me₁₀CB[5])][PdCl₄] (**5**): Yield: ≈45%, based on Me₁₀CB[5]; elemental analysis calcd (%) for C₄₀H₅₆N₂₀O₁₃Cl₄Cs₂Pd: C: 31.3, H: 3.63, N: 19.4; found: C: 31.2, H: 3.64, N: 18.2.

Application as catalysts in the Heck reaction: *General procedure for the Heck coupling reaction:* A mixture of aryl halide (1 mmol, 1 equiv), alkene (1.5 mmol, 1.5 equiv), sodium carbonate (2 mmol, 2 equiv), and a Pd catalyst (1.0 mol%) in DMF (3 mL) was stirred in a 15 mL pressure tube at 140 °C for 24 h. At the end of each reaction, the Pd catalyst was separated by centrifugation, and the filtrate was diluted with water followed by extraction with ethyl acetate (3×10 mL). The combined organic phase was dried over anhydrous Na₂SO₄. After removal of the solvent, the crude product was directly analyzed by GC. The product was further transferred to column chromatography on silica gel using petroleum ether to afford the product with high purity. ¹H NMR (400 MHz) and ¹³C NMR (100 MHz) spectra were recorded in CDCl₃ solution. Recovery of the M–Pd–Me₁₀CB[5] (M=K, Rb, and Cs) catalysts were separated by centrifugation after the first run and washed to remove inorganic salt and adsorbed organic substrate, followed by drying at 40 °C. Then, the catalysts were used for the second run without further activation and similar processes were repeated for the next runs.

Acknowledgements

We thank the financial support from the 973 Program (2011CB932504 and 2012CB821705), NSFC (21221001, 21101155, and 21001105), Fujian Key Laboratory of Nanomaterials (2006L2005) and the Key Project from CAS. J.L. gratefully acknowledges the financial support from NSFC-RS for the International Exchanges Scheme (2011 China Costshare project based on 21001105) and the Royal Society Sino-British Fellowship Trust for an Incoming Fellowship. We are grateful to Prof. Xiaoying Huang from FJIRSM for the structural analyses.

- [1] a) N. T. S. Phan, M. Van Der Sluys, C. W. Jones, *Adv. Synth. Catal.* **2006**, *348*, 609–679; b) R. F. Heck, *Org. React.* **1982**, *27*, 345–390; c) J. P. Wolfe, S. L. Buchwald, *Angew. Chem.* **1999**, *111*, 2570–2573; d) J. P. Wolfe, R. A. Singer, B. H. Yang, S. L. Buchwald, *J. Am. Chem. Soc.* **1999**, *121*, 9550–9561.
- [2] a) R. B. Bedford, *Chem. Commun.* **2003**, 1787–1796; b) J. Dupont, M. Pfeffer, J. Spencer, *Eur. J. Inorg. Chem.* **2001**, 1917–1927; c) A. H. M. de Vries, F. J. Parlevliet, L. Schmieder-van de Vondervoort, J. H. M. Mommers, H. J. W. Henderickx, M. A. M. Walet, J. G. de Vries, *Adv. Synth. Catal.* **2002**, *344*, 996–1002; d) A. H. M. de Vries, J. M. C. A. Mulders, J. H. M. Mommers, H. J. W. Henderickx, J. G. de Vries, *Org. Lett.* **2003**, *5*, 3285–3288; e) M. T. Reetz, E. Westermann, R. Lohmer, G. Lohmer, *Tetrahedron Lett.* **1998**, *39*, 8449–8452.
- [3] M. Tromp, J. R. A. Sielsma, J. A. van Bokhoven, G. P. F. Van Strijdonck, R. J. Van Haaren, A. M. J. van der Eerden, P. W. N. M. Van Leeuwen, D. C. Koningsberger, *Chem. Commun.* **2003**, 128–129.
- [4] a) E. Peris, R. H. Crabtree, *Coord. Chem. Rev.* **2004**, *248*, 2239–2246; b) R. B. Bedford, C. S. J. Cazin, D. Holder, *Coord. Chem. Rev.* **2004**, *248*, 2283–2321; c) N. Marion, S. Diez-González, S. P. Nolan, *Angew. Chem.* **2007**, *119*, 3046–3058; *Angew. Chem. Int. Ed.* **2007**, *46*, 2988–3000; d) F. E. Hahn, M. C. Jahnke, *Angew. Chem.* **2008**, *120*, 3166–3216; *Angew. Chem. Int. Ed.* **2008**, *47*, 3122–3172.
- [5] a) E. Alcalde, R. M. Ceder, C. López, N. Mesquida, G. Muller, S. Rodríguez, *Dalton Trans.* **2007**, 2696–2706; b) N. Marion, R. S. Ramón, S. P. Nolan, *J. Am. Chem. Soc.* **2009**, *131*, 448–449; c) D. G. Gusev, *Organometallics* **2009**, *28*, 763–770; d) P. V. Sashuk, D. Schoeps, H. Plenio, *Chem. Commun.* **2009**, 770–772; e) N. Marion, O. Navarro, J. Mei, E. D. Stevens, N. M. Scott, S. P. Nolan, *J. Am. Chem. Soc.* **2006**, *128*, 4101–4111.
- [6] a) D. Kremzow, G. Seidel, C. W. Lehmann, A. Fuerstner, *Chem. Eur. J.* **2005**, *11*, 1833–1853; b) X. M. Zhang, Q. Q. Xia, W. Z. Chen, *Dalton Trans.* **2009**, 7045–7054; c) B. Lin, Q. Q. Xia, W. Z. Chen, *Angew. Chem.* **2009**, *121*, 5621–5624; *Angew. Chem. Int. Ed.* **2009**, *48*, 5513–5516; d) M. Delamplé, N. Villandier, J.-P. Douliet, S. Camy, J.-S. Condoret, Y. Pouilloux, J. Barrault, F. Jérôme, *Green Chem.* **2010**, *12*, 804–808; e) H. Yang, Y. Wang, Y. Qin, Y. Chong, Q. Yang, G. Li, L. Zhang, W. Li, *Green Chem.* **2011**, *13*, 1352–1391.
- [7] a) M. Poyatos, J. A. Mata, E. Peris, *Chem. Rev.* **2009**, *109*, 3677–3707; b) B. P. Morgan, G. A. Galdamez, R. J. Gilliard Jr., R. C. Smith, *Dalton Trans.* **2009**, 2020–2028; c) T. H. Hsiao, T. L. Wu, S. Chatterjee, C. Y. Chiu, H. M. Lee, L. Bettucci, C. Bianchini, W. Oberhauser, *J. Organomet. Chem.* **2009**, *694*, 4014–4024; d) A. Biffis, C. Tubaro, G. Buscemi, M. Basato, *Adv. Synth. Catal.* **2008**, *350*, 189–196; e) C. Tubaro, A. Biffis, C. Gonzato, M. Zecca, M. Basato, *J. Mol. Catal. A: Chem.* **2006**, *248*, 93–98.
- [8] L. Li, J. Wang, C. Zhou, R. Wang, M. Hong, *Green Chem.* **2011**, *13*, 2071–2077.
- [9] a) R. Behrend, E. Meyer, F. Rusche, *Justus Liebigs Ann Chem.* **1905**, 339, 1–37; b) W. A. Freeman, W. L. Mock, N.-Y. Shih, *J. Am. Chem. Soc.* **1981**, *103*, 7367–7368; c) J. Kim, I.-S. Jung, S.-Y. Kim, E. Lee, J.-K. Kang, S. Sakamoto, K. Yamaguchi, K. Kim, *J. Am. Chem. Soc.* **2000**, *122*, 540–541; d) A. I. Day, A. P. Arnold, R. J. Blanch, B. Snushall, *J. Org. Chem.* **2002**, *67*, 8094–8100.
- [10] X. Lu, E. Masson, *Langmuir* **2011**, *27*, 3051–3058.
- [11] J. Lü, J. X. Lin, M. N. Cao, R. Cao, *Coord. Chem. Rev.* **2013**, *257*, 1334–1356.

- [12] a) J. Lin, J. Lü, M. Cao, R. Cao, *Cryst. Growth Des.* **2011**, *11*, 778–783; b) Y. Q. Zhang, L. M. Zhen, D. H. Yu, Y. J. Zhao, S. F. Xue, Q. J. Zhu, Z. Tao, *J. Mol. Struct.* **2008**, *875*, 435–441; c) D. G. Samsonenko, A. A. Sharonova, M. N. Sokolov, A. V. Virovets, V. P. Fedin, *Koord. Khim.* **2001**, *27*, 10–15 [*Russ. J. Coord. Chem.* **2001**, *27*, 10–15 (Engl. Transl.)]; d) D. G. Samsonenko, O. A. Gerasko, T. V. Mitkina, J. Lipkowski, A. V. Virovets, D. Fenske, V. P. Fedin, *Koord. Khim.* **2003**, *29*, 166–174; [*Russ. J. Coord. Chem.* **2003**, *29*, 166–174 (Engl. Transl.)]; e) O. A. Gerasko, E. A. Mainicheva, D. Yu Naumov, V. P. Fedin, *Russ. Chem. Bull.* **2007**, *56*, 1972–1977.
- [13] a) A. A. Tripol'skaya, E. A. Mainicheva, O. A. Geras'ko, D. Yu Naumov, V. P. Fedin, *J. Struct. Chem.* **2007**, *48*, 547–551; b) J. X. Liu, L. S. Long, R. B. Huang, L. S. Zheng, *Inorg. Chem.* **2007**, *46*, 10168–10173; c) P. Thuéry, *Inorg. Chem.* **2009**, *48*, 4497–4499; d) D. G. Samsonenko, J. Lipkowski, O. A. Gerasko, A. V. Virovets, M. N. Sokolov, V. P. Fedin, J. G. Platas, R. Hernandez-Molina, A. Mederos, *Eur. J. Inorg. Chem.* **2002**, *9*, 2380–2388; e) P. Thuéry, *Cryst. Growth Des.* **2011**, *11*, 2606–2620.
- [14] a) J. Lagona, P. Mukhopadhyay, S. Chakrabarti, L. Isaacs, *Angew. Chem.* **2005**, *117*, 4922–4949; *Angew. Chem. Int. Ed.* **2005**, *44*, 4844–4870; b) O. A. Gerasko, V. P. Fedin, *Russ. J. Inorg. Chem.* **2011**, *56*, 2025–2046; c) J. W. Lee, S. Samal, N. Selvapalam, H.-J. Kim, K. Kim, *Acc. Chem. Res.* **2003**, *36*, 621–630; d) A. E. Rowan, J. A. A. W. Elemans, R. J. M. Nolte, *Acc. Chem. Res.* **1999**, *32*, 995–1006; e) A. Suvitha, N. S. Venkataramanan, H. Mizuseki, Y. Kawazoe, N. Ohuchi, *J. Inclusion Phenom. Macrocyclic Chem.* **2010**, *66*, 213–218.
- [15] E. Masson, X. Ling, R. Joseph, L. Kyeremeh-Mensah, X. Lu, *RSC Adv.* **2012**, *2*, 1213–1247.
- [16] a) S. M. de Lima, J. A. Gómez, V. P. Barros, G. de S. Vertuan, M. das D. Assis, C. F. de O. Graeff, G. J.-F. Demets, *Polyhedron* **2010**, *29*, 3008–3013; b) E. A. Karakhanov, L. M. Karapetyan, Y. S. Kardasheva, A. L. Maksimov, E. A. Runova, M. V. Terenina, T. Y. Philippova, *Macromol. Symp.* **2008**, *270*, 106–116; c) X. Lu, E. Masson, *Org. Lett.* **2010**, *12*, 2310–2313.
- [17] A. Flinn, G. C. Hough, J. F. Stoddart, D. J. Williams, *Angew. Chem.* **1992**, *104*, 1550–1551; *Angew. Chem. Int. Ed. Engl.* **1992**, *3*, 1475–1477.
- [18] J. X. Liu, L. S. Long, R. B. Huang, L. S. Zheng, *Cryst. Growth Des.* **2006**, *6*, 2611–2614.
- [19] a) T. Mizoroki, K. Mori, A. Ozaki, *Bull. Chem. Soc. Jpn.* **1971**, *44*, 581–583; b) R. F. Heck, J. P. Nolley, *J. Org. Chem.* **1972**, *37*, 2320–2322.
- [20] a) K. Yu, W. Sommer, J. M. Richardson, M. Weck, C. W. Jones, *Adv. Synth. Catal.* **2005**, *347*, 161–171; b) J. Vignolle, T. D. Tilley, *Chem. Commun.* **2009**, 7230–7232; c) J. Zhou, X. Y. Li, H. J. Sun, *J. Organomet. Chem.* **2010**, *695*, 297–303.
- [21] M. T. Reetz, J. G. de Vries, *Chem. Commun.* **2004**, 1559–1563.
- [22] a) M. T. Reetz, M. Maase, *Adv. Mater.* **1999**, *11*, 773–777; b) M. T. Reetz, R. Breinbauer, K. Wanninger, *Tetrahedron Lett.* **1996**, *37*, 4499–4502; c) M. Beller, H. Fischer, K. Kühlein, C.-P. Reisinger, W. A. Herrmann, *J. Organomet. Chem.* **1996**, *520*, 257–259; d) M. T. Reetz, G. Lohmer, *Chem. Commun.* **1996**, 1921–1922; e) C. Rocaboy, J. A. Gladysz, *New J. Chem.* **2003**, *27*, 39–49; f) M. T. Reetz, E. Westermann, *Angew. Chem.* **2000**, *112*, 170–173; *Angew. Chem. Int. Ed.* **2000**, *39*, 165–167.
- [23] a) M. T. Reetz, R. Breinbauer, P. Wedemann, P. Binger, *Tetrahedron* **1998**, *54*, 1233–1240; b) M. Moreno-Mañas, R. Pleixats, *Acc. Chem. Res.* **2003**, *36*, 638–643; c) A. Biffis, M. Zecca, M. Basato, *J. Mol. Catal. A: Chem.* **2001**, *173*, 249–274; d) A. Roucoux, J. Schulz, H. Patin, *Chem. Rev.* **2002**, *102*, 3757–3778; e) C. C. Cassol, A. P. Umpierre, G. Machado, S. I. Wolke, J. Dupont, *J. Am. Chem. Soc.* **2005**, *127*, 3298–3299.
- [24] a) A. Balanta, C. Godard, C. Claver, *Chem. Soc. Rev.* **2011**, *40*, 4973–4985; b) V. Polshettiwar, C. Len, A. Fihri, *Coord. Chem. Rev.* **2009**, *253*, 2599–2626; c) X. R. Ye, Y. Lin, C. M. Wai, *Chem. Commun.* **2003**, 642–643; d) R. Bernini, S. Cacchi, G. Fabrizi, G. Forte, F. Petrucci, A. Prastaro, S. Niembro, A. Shafir, A. Vallribera, *Green Chem.* **2010**, *12*, 150–158; e) F. Z. Su, Y. M. Liu, Y. Cao, K. N. Fan, *Angew. Chem.* **2008**, *120*, 340–343; *Angew. Chem. Int. Ed.* **2008**, *47*, 334–337.
- [25] a) M. Cao, D. Wu, S. Gao, R. Cao, *Chem. Eur. J.* **2012**, *18*, 12978–12985; b) M. Cao, J. Lin, H. Yang, R. Cao, *Chem. Commun.* **2010**, *46*, 5088–5090; c) M. Cao, Y. Wei, S. Gao, R. Cao, *Catal. Sci. Technol.* **2012**, *2*, 156–163; d) T. Premkumar, Y. Lee, K. E. Geckeler, *Chem. Eur. J.* **2010**, *16*, 11563–11566; e) A. Corma, H. Garía, P. M. Navajas, A. Primo, J. J. Calvino, S. Trasobares, *Chem. Eur. J.* **2007**, *13*, 6359–6364; f) T.-C. Lee, O. A. Scherman, *Chem. Commun.* **2010**, *46*, 2438–2440.
- [26] N.-Y. Shih, *Diss. Abst. Int.* **1982**, *B42*, 4071.
- [27] G. M. Sheldrick, *SADABS*, University of Göttingen: Göttingen, Germany, **1996**.
- [28] SHELXTL, *version 5.10*, Siemens Analytical X-ray Instruments Inc., Madison, WI, **1994**.

Received: May 3, 2013
Revised: August 7, 2013
Published online: October 7, 2013